Downlink Probability Density Functions for EOS-McMurdo Sound

P. Christopher
Stanford Telecom
Reston, VA

A. H. Jackson
Goddard Space Flight Center (GSFC)
Greenbelt, MD

Abstract

The visibility times and communication link dynamics for the EOS-McMurdo Sound direct downlinks have been studied recently. The 16-day EOS periodicity may be shown with the Goddard Trajectory Determination System (GTDS), and the entire 16-day period should be simulated for representative link statistics. We desire many attributes of the downlink, however, and a faster orbital determination method is desirable. We use the method of osculating elements for speed and accuracy in simulating the EOS orbit. The accuracy of the method of osculating elements is demonstrated by closely reproducing the observed 16-day Landsat periodicity. An autocorrelation function method is used to show the correlation spike at 16 days.

The entire 16-day record of passes over McMurdo Sound is then used to generate statistics for innage time, outage time, elevation angle, antenna angle rates, and propagation loss. The elevation angle probability density function is compared with a 1967 analytic approximation which has been used for medium to high altitude satellites. One practical result of this comparison is seen to be the rare occurrence of zenith passes. The new result is functionally different than the earlier result, with a heavy emphasis on low elevation angles. EOS is one of a large class of sun synchronous satellites which may be downlinked to McMurdo Sound. We examine delay statistics for an entire group of sun synchronous satellites ranging from 400 km to 1000 km altitude. Outage probability density function results are presented three dimensionally.

1. Introduction

A new series of environmental spacecraft, such as the Earth Observation Satellite (EOS), may use the Tracking and Data Relay Satellite System (TDRSS) in some unique ways. Polar orbiting environmental spacecraft spend an appreciable portion of their orbit over the poles. The polar orbit of EOS or of Landsat may be represented as in Figure 1-1. The individual views are taken as a series of snapshots at 8.2 minute intervals. It is seen to be slightly retrograde, with a 98-degree inclination. EOS and other environmental spacecraft may find it more convenient to downlink their data directly to a ground station in Antarctica rather than relaying it over a distance of six earth radii to a geosynchronous relay. We examine these downlinks in some detail.

A ground station at McMurdo Sound, Antarctica has been constructed by NASA to answer these needs. A polar satellite such as an Earth Observation Satellite (EOS) would be able to link to McMurdo Sound in a visibility region as shown in Figure 1-2. McMurdo would then uplink to TDRS West, to complete the link to the White Sands Complex (WSC).

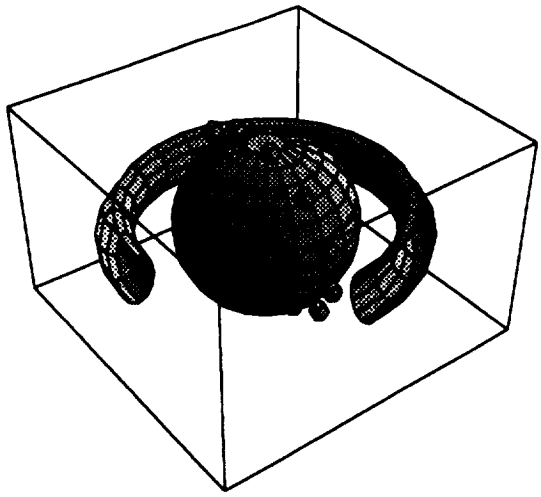

Figure 1-1: Inclined Landsat (EOS) Orbit Inside VanAllen Belt

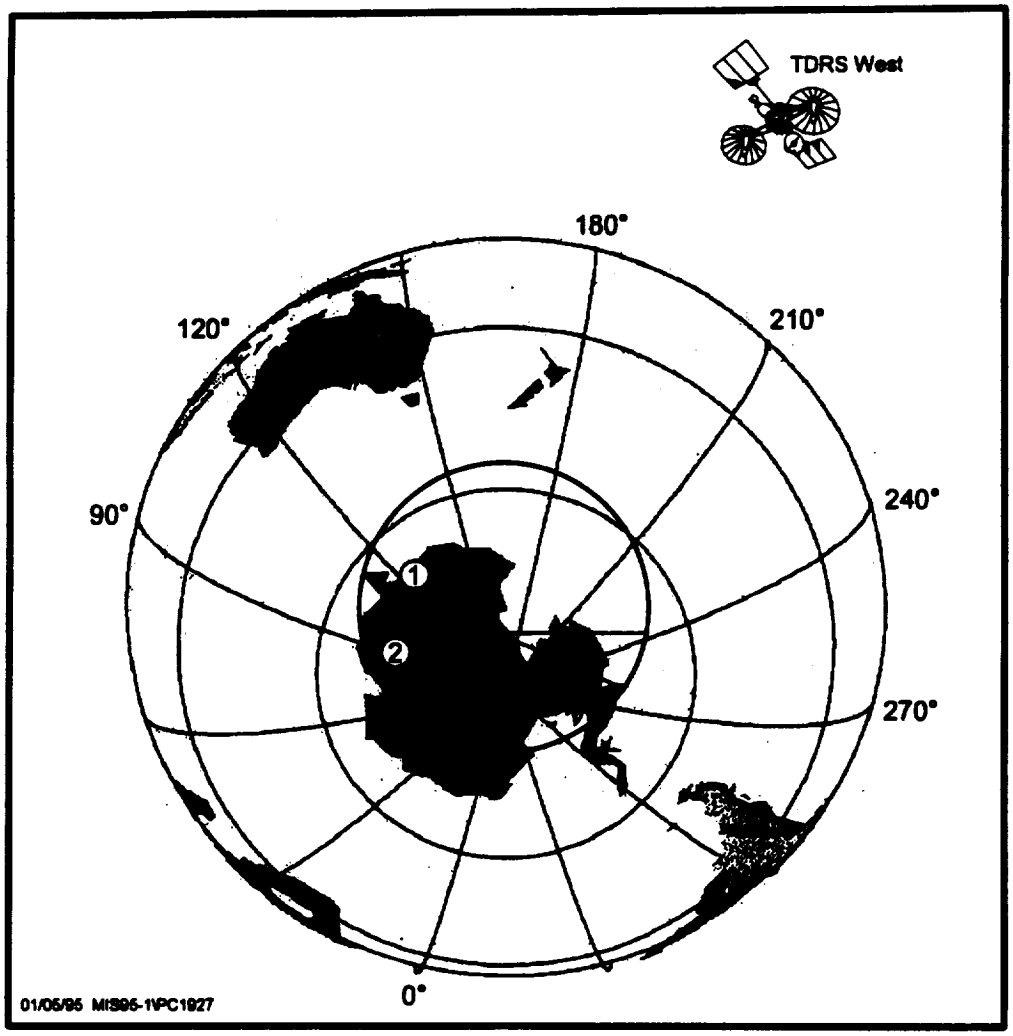

Note the first EOS pass, labelled (1).

Figure 1-2: McMurdo Sound-EOS Visibility Region Radius 25.6°

We address some of the communication link dynamics for the user satellite pass over McMurdo Sound. Sun synchronous satellites will be of widespread interest, and we closely examine arrival times, departure times, and atmospheric signal loss as a function of time during the pass over the ground station. These data may be further examined to generate interarrival time statistics, link duration statistics, and signal loss statistics as an aid to the system designer. EOS, as a clearly important member of the class of sun synchronous satellites, gets special attention.

Many long computer simulations are necessary for this report. The method of osculating orbits (1) is used here for speed and accuracy. The oblate earth perturbation terms are vital to descriptions of the 16-day EOS periodicity. Indeed, the 16-day periodicity can be used as a simulation check against existing Landsat4 data. Most of our EOS runs include the entire 16-day periodic interval as a key check. However, only small portions of the output tables are included here because of space limits. The report begins with a brief description of oblate earth perturbation terms which are necessary for the method of osculating elements.

Atmospheric attenuation on the McMurdo-satellite link is closely related to the orbital computations because the attenuation depends strongly on the ground station elevation angle. We use two new attenuation results as an integral part of the orbital program. The first new propagation result is due to Liebe (2). The new propagation results are used but not included because of space limitations. A short portion of a long EOS simulation follows. The long-term EOS statistics are included as a way to keep the results brief. General sun synchronous results conclude the report. Sun synchronous altitudes between 400-1000 km will be seen to offer short interarrival times at McMurdo Sound, but altitudes below 500 km will occasionally skip an orbit before visibility repeats.

Appendix A condenses the long 16 day simulation into short graphical output.

2.0 Analysis

The anticipated long 16-day periodicity of EOS leads us to consider methods to reproduce the entire 16-day period with suitable accuracy. Anything less would cause serious doubts about the ground elevation statistics and the propagation loss studies which follow. The method of osculating elements, with analytic approximations for the perturbed motion, is useful for fast and relatively accurate orbit prediction for missions of long duration. Moulton (3) gives the basis of the method as the partial derivatives of the instantaneous orbital elements as a function of a perturbing potential. Brouwer (4), Kozai (5), and Blitzer (6) have used the method to achieve exhaustive insights into the motion of low earth orbiting satellites. Their results for satellite perturbations may be subdivided into secular components, long cycle components, and short cycle components. We desire only the secular components here, and omit the long and short cycle terms because they tend to cancel out their effects over the long term. Omission of the short cycle component has implied a maximum instantaneous orbital error of a few kilometers for the 1958 Vanguard orbit. We accept that error, along with the error due to lunar perturbations (although lunar perturbations can be included with the method of osculating elements with the aid of results by Ash (1)).

The key secular terms are:

$$\dot{W} = \frac{1}{a}\sqrt{\frac{u}{a}}\left\{ -\frac{3}{2}J_2\left(\frac{R}{P}\right)^2 cos(i) + \frac{3}{32}J_2^2\left(\frac{R}{P}\right)^4 \right.$$
$$\bullet\left[(4+12\sqrt{1-e^2}-9e^2)cos(i)+(-40-36\sqrt{1-e^2}+5e^2)cos^3(i)\right] \qquad 2\text{-}1$$
$$\left. -\frac{15}{32}J_4\left(\frac{R}{P}\right)^4 (2+3e^2)(3-7cos^2(i))cos(i) \right\} \qquad Rad/Sec$$

$$\dot{W}_P = \frac{1}{a}\sqrt{\frac{u}{a}}\left\{\frac{3}{4}J_2\left(\frac{R}{P}\right)^2(-1+5\cos^2(i)) + \frac{3}{128}J_2^2\left(\frac{R}{P}\right)^4 \right.$$
$$\bullet\left[-10+24\sqrt{1-e^2}-25e^2+(-36-192\sqrt{1-e^2}+126e^2)\cos^2(i)\right.$$
$$\left.+(430+360\sqrt{1-e^2}-45e^2)\cos^4(i)\right] \qquad 2\text{-}2$$
$$-\frac{45}{128}J_4\left(\frac{R}{P}\right)^4\left[12+9e^2+(-144-126e^2)\cos^2(i)\right.$$
$$\left.\left.+(196+189e^2)\cos^4(i)\right]\right\} \qquad Rad/Sec$$

$$\dot{M} = \frac{1}{a}\sqrt{\frac{u}{a}}\left\{1+\frac{3}{4}J_2\left(\frac{R}{P}\right)^2\sqrt{1-e^2}(-1+3\cos^2(i)) + \frac{3}{128}J_2^2\left(\frac{R}{P}\right)^4\sqrt{1-e^2}\right.$$
$$\bullet\left[10+16\sqrt{1-e^2}-25e^2+(-60-96\sqrt{1-e^2}+90e^2)\cos^2(i)\right.$$
$$\left.+(130+144\sqrt{1-e^2}-25e^2)\cos^4(i)\right] - \frac{45}{128}J_4\left(\frac{R}{P}\right)^4\sqrt{1-e^2} \qquad 2\text{-}3$$
$$\left.\bullet(3-30\cos^2(i)+35\cos^4(i))\right\} \qquad Rad/Sec$$

with the key variables defined below

The method of osculating orbital elements allows the Keplerian orbital elements to be continuously updated without concern for the time interval between updates. It also offers a concise orbital description, which allows other important satellite communication features such as link propagation to be included in the same computer code.

The secular perturbations may be abbreviated further, while usually retaining over 99% of the accuracy of the secular terms. The oblateness effects have been found to give a regression of nodes

$$\dot{W} = -\frac{3}{2a}\sqrt{\frac{u}{a}}J_2\left(\frac{R}{P_L}\right)^2 \cos(i)\ rad/sec \qquad 2\text{-}4$$

The argument of perigee changes as

$$\dot{W}_P = \frac{3}{4a}\sqrt{\frac{u}{a}}J_2\left(\frac{R}{P_L}\right)^2 (-1+5\cos^2(i))\ rad/sec \qquad 2\text{-}5$$

and the mean anomaly changes as

$$\dot{M} = \frac{3}{4a}\sqrt{\frac{u}{a}}J_2\left(\frac{R}{P}\right)^2 \sqrt{1-e^2}(-1+3\cos^2(i))\ rad/sec \qquad 2\text{-}6$$

W = right ascension. rad

W_P = argument of perigee, rad

R = earth radius, km

Where

μ = earth gravitational constant

= $0.39860064 * 10^6$ km^3/sec^2

P = a (1-e^2) = semilatus rectum

J_2 = $1.082635 * 10^{-3}$

e = eccentricity

i = inclination, rad.

3.0 EOS Simulation Results

Table 3-1 indicates a first pass (labeled 1) of EOS over the McMurdo Sound ground station. It uses 1992 Landsat4 orbital elements. Table 3-1 lists the first and second passes in an abbreviated simulation output. Elevation angle, attenuation, and subsatellite point are listed as a function of time for the EOS passes. The first attenuation column is for a single link, and the second represents a dual switched link. Attenuation is chosen at the 0.997 precipitation probability level for a 1.0 km altitude precipitation layer (7,9). The subsatellite point is recognized as North Latitude and East Longitude. Time is in hours from start of the Epoch (note 1 minute increments). Range is in megameters.

Table 3-1: EOS Downlinked to Antarctica

EOS DOWNLINKED TO ANTARCTICA TAVG(K)= 201
EOS LINK ; X BAND GND SITE-78.11 166.2272 GFHZ= 8.2875E+09
RP PREC.RATE(MM/HR) = 1.498039 AVAIL= .997 PRECIP. HT.= 1
A,E,I= 7077.79 .0014055 98.39766
MASK ANGLE= 1 DEG

I	ELEV	(SINGLE,	DUAL,	CLEAR A)	NLAT	ELON	TIME	RANG,MM
1.000	1.079	3.592	2.756	2.219	-69.334	263.313	1.150	2.989
2.000	5.205	0.897	0.702	0.612	-72.583	258.031	1.167	2.582
3.000	10.174	0.440	0.350	0.315	-75.652	250.604	1.183	2.179
4.000	16.527	0.265	0.213	0.195	-78.396	239.637	1.200	1.785
5.000	25.313	0.172	0.140	0.130	-80.528	223.122	1.217	1.408
6.000	38.572	0.115	0.095	0.089	-81.569	200.274	1.233	1.071
7.000	58.628	0.081	0.068	0.065	-81.124	175.823	1.250	0.825
8.000	68.386	0.073	0.062	0.060	-79.380	156.536	1.267	0.765
9.000	47.904	0.095	0.079	0.075	-76.841	143.511	1.283	0.929
10.000	31.266	0.140	0.114	0.107	-73.880	134.820	1.300	1.230
11.000	20.539	0.212	0.172	0.158	-70.688	128.769	1.317	1.591
12.000	13.127	0.337	0.269	0.245	-67.364	124.337	1.333	1.978
13.000	7.543	0.604	0.476	0.423	-63.957	120.938	1.350	2.378
14.000	3.036	1.598	1.238	1.049	-60.496	118.227	1.367	2.783
15.000	2.627	1.868	1.443	1.212	-66.368	242.138	2.783	2.835
16.000	6.994	0.654	0.515	0.456	-69.714	238.066	2.800	2.432
17.000	12.329	0.360	0.287	0.260	-72.947	232.587	2.817	2.036
18.000	19.251	0.226	0.183	0.169	-75.988	224.838	2.833	1.653
19.000	28.865	0.151	0.123	0.115	-78.680	213.341	2.850	1.298
20.000	42.619	0.105	0.087	0.082	-80.714	196.072	2.867	1.004
21.000	57.172	0.082	0.069	0.066	-81.596	172.672	2.883	0.837
22.000	52.827	0.088	0.073	0.070	-80.981	148.547	2.900	0.875
23.000	37.117	0.119	0.098	0.092	-79.119	130.029	2.917	1.097
24.000	24.921	0.174	0.142	0.132	-76.517	117.610	2.933	1.419
25.000	16.414	0.267	0.215	0.197	-73.522	109.294	2.950	1.786
26.000	10.144	0.441	0.351	0.315	-70.311	103.472	2.967	2.175
27.000	5.200	0.898	0.702	0.613	-66.975	99.182	2.983	2.574
28.000	1.081	3.592	2.756	2.219	-63.561	95.876	3.000	2.979

Elevation Angles at McMurdo

The time variation of elevation of EOS or Landsat over McMurdo Sound may be seen with some elevation and attenuation plots. The first satellite pass over McMurdo may be seen in the lower left corner of Figure 3-1. Elevation is shown with data points, and the corresponding atmospheric attenuation of a hypothetical 27 GHz link is shown with a solid line. The data points are chosen at one minute intervals, and most passes are seen to be limited to less than 10 minutes. The long period between passes is taken out of the figure so that almost two days of satellite passes may be fitted onto the figure. The passes are seen to group as several high passes followed by a group of very low passes barely above the assumed 5 degree mask. The simulated elevation after 16 days is shown in the following figure (Figure 3-2). The figure is strikingly similar to that for the initial passes, but other methods should be used to confirm a true 16-day periodicity.

Figure 3-3 shows the result of an autocorrelation of the entire 21.75-day elevation simulation with itself. The autocorrelation peaks at 1.0 when the series is cross correlated with itself for zero phase delay. It is seen to have a cyclic correlation with later passes. As the lag times get longer, the cross correlation is rarely over 0.4 until the lag time is set at 16 days (Figure 3-4) when the autocorrelation peaks at over 0.7. Longer phase differences also match the initial autocorrelation function (labeled Rx) well, but not perfectly.

Elevation Probability Density Functions

Elevation angle probability density functions (pdfs) have been interesting and important since the early '60s. Lutz and Dorosheski (9) recognized that satellite ground station economics depended on the ground station elevation angles. They looked at the entire ensemble of ground stations seen by a geosynchronous satellite, and treated the ensemble of elevation angles as a pdf. Sugai and Christopher (10) derived a simpler pdf which was useful for medium altitude to geosynchronous orbits. The simpler pdf was of the form:

$$p(E) = \frac{\left(\frac{\pi}{180}\right)\cos\left(\frac{\pi}{180}E\right)\left(1 - 2s\,\sin\left(\frac{\pi}{180}E\right)\right)}{\left(1 - s\,\cos^2\left(\frac{\pi}{36}\right) - \sin\left(\frac{\pi}{36}\right)\right)} \qquad 3\text{-}1$$

Where

E = elevation, deg.

E_{min} = minimum elevation, deg. = 5°

s = earth radius/semimajor axis = 1/6.6227 for geo satellite

Figure 3-5 shows the emphasis on low elevation angle for the pdf generated by equation 3-1 for Geo altitudes. However, the 16-day simulation of Landsat4 passes over McMurdo Sound and shows an entirely different emphasis on low elevation angles, as seen in Figure 3-6. A fit for the McMurdo elevation pdf may be found as:

$$p(E) = 0.00064269\,\csc^2\left(\frac{\pi}{180}E\right) + \frac{0.003228\,\pi\cos\left(\frac{\pi}{180}E\right)\left(1 - 1.087\sin\left(\frac{\pi}{180}E\right)\right)}{\left(1 - 0.5435\,\cos^2\left(\frac{\pi}{36}\right) - \sin\left(\frac{\pi}{36}\right)\right)} \qquad 3\text{-}2$$

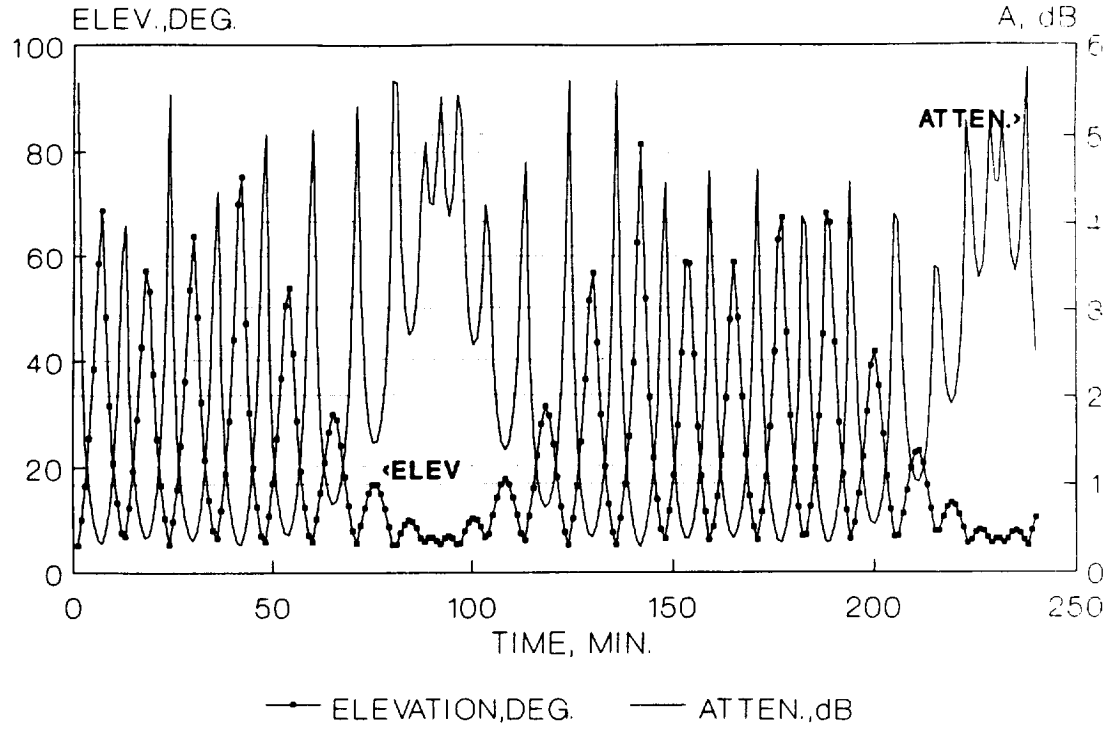

Figure 3-1: Elevation for McMurdo-EOS for Successive Passes

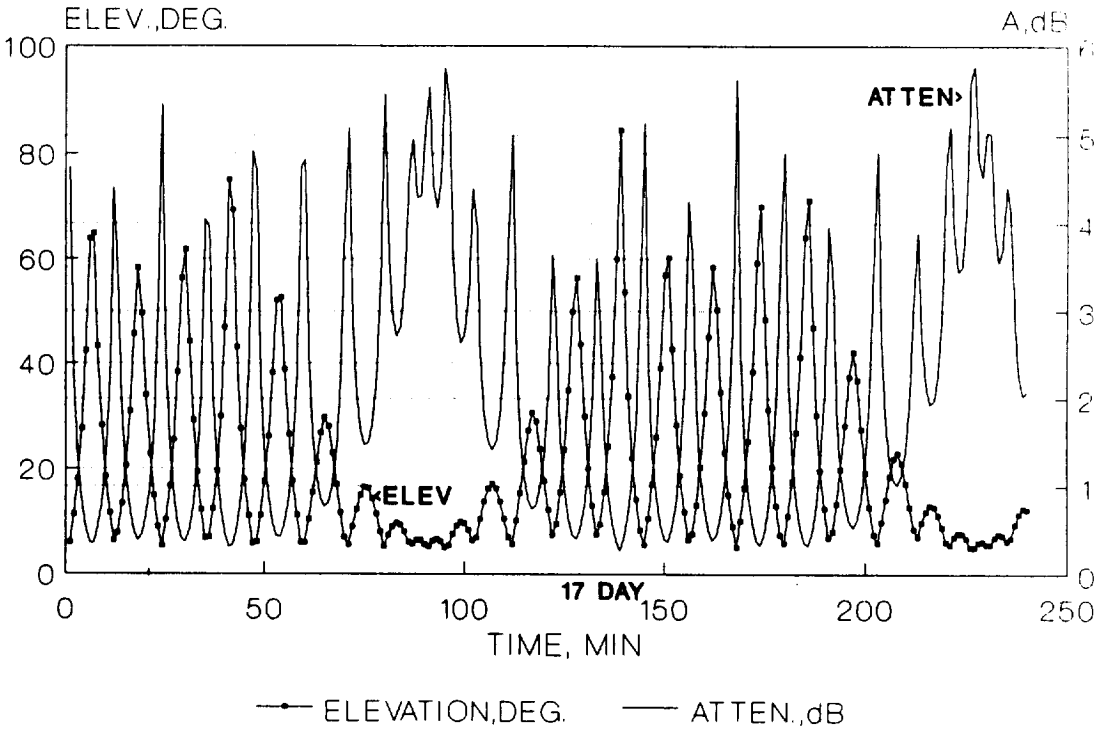

Figure 3-2: Elevation at 16 Days for McMurdo-EOS

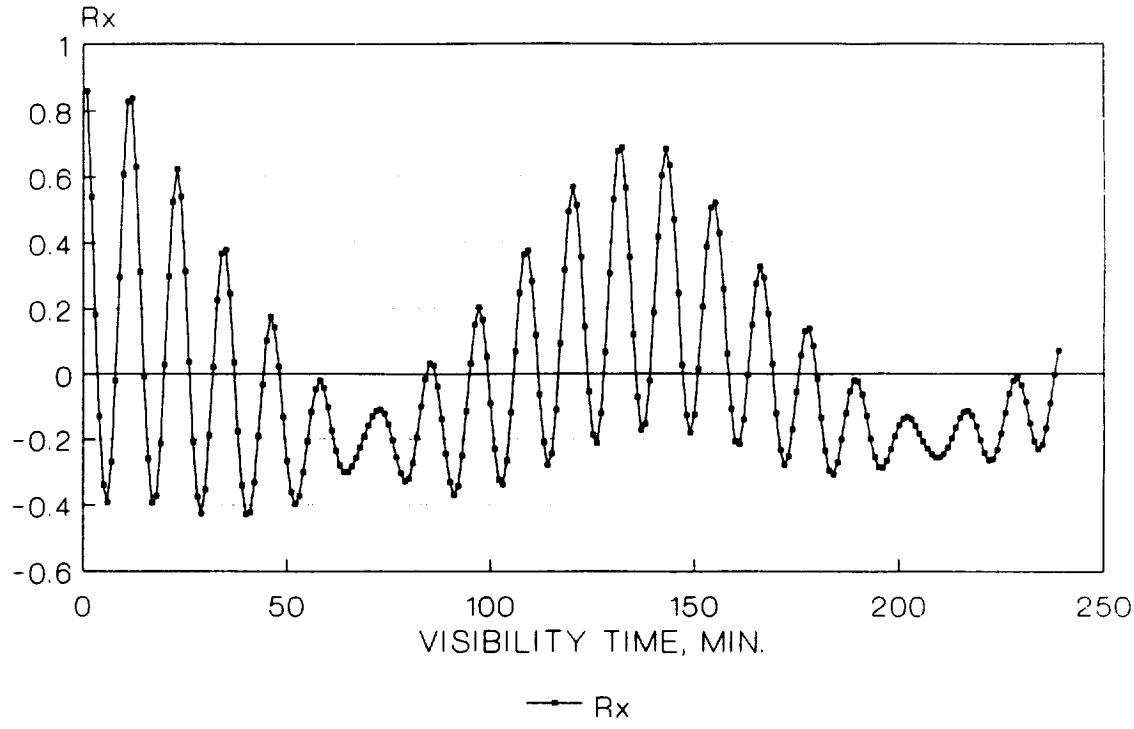

Figure 3-3: Elevation Autocorrelation vs. Lag Time, Min.

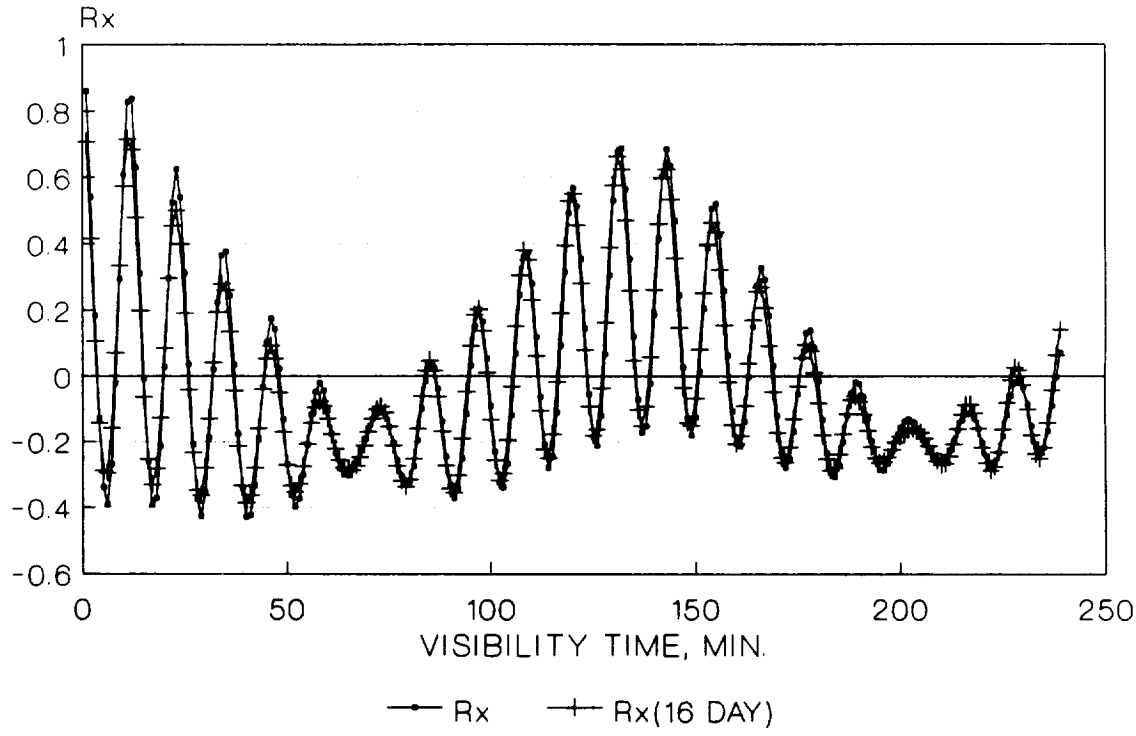

Figure 3-4: Elevation Autocorrelation Compared to 16-Day Autocorrelation

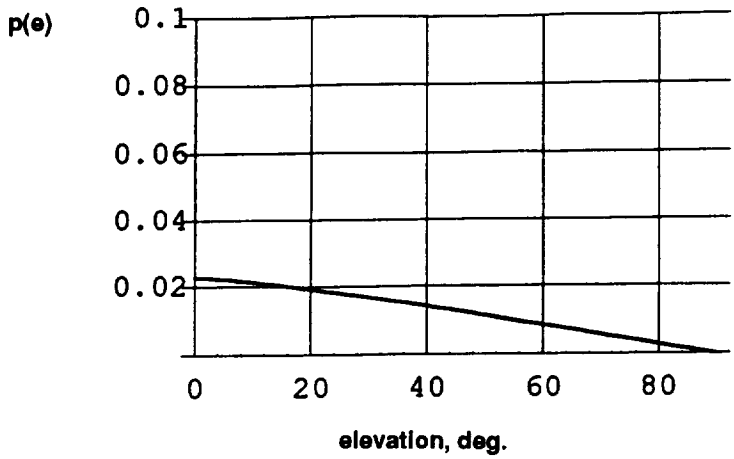

Figure 3-5: Ground Elevation Probability Density Function to Geosynchronous Satellite

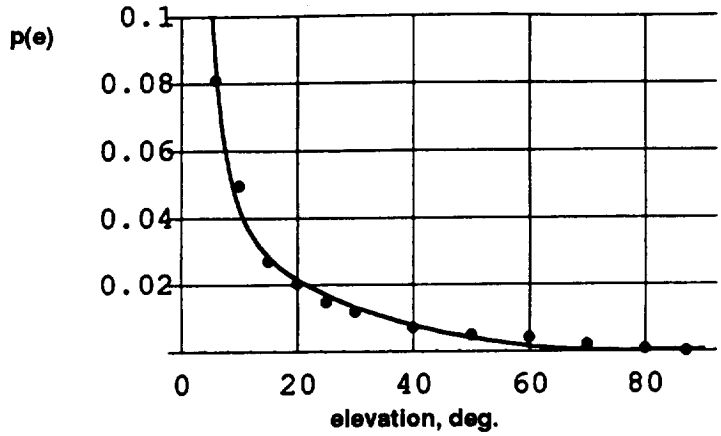

Figure 3-6: Elevation PDF for McMurdo Sound-EOS

Equation 3-2 is compared with the McMurdo data in Figure 3-7. It is useful, because it emphasizes the importance of the ground site's ability to acquire Landsat or EOS quickly at the horizon. The overall communication time available increases sharply if the minimum elevation at the ground site can be 3 deg., for example, rather than 5 deg.

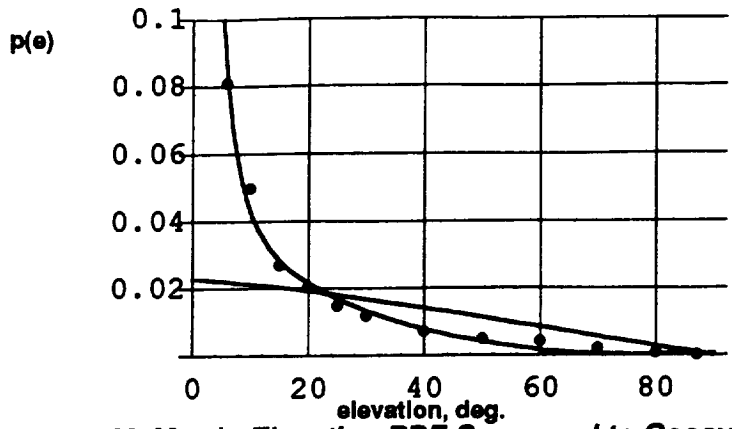

Figure 3-7: McMurdo Elevation PDF Compared to Geosynchronous PDF

Appendix A shows the full 16-day periodicity of actual Landsat 4 elements (assumed to be identical to EOS elements here). The interarrival interval statistics and other link statistics may be summarized as in Table 3-2.

Table 3-2: EOS Downlink Statistics to McMurdo Sound

F = 8.28 GHz Precipitation Height = 1.0 km 0.997 Availability

	Mean	Standard Deviation	Maximum
in view, hr (min)	0.1848 (11.08)	0.032 (1.92)	0.2167 (13.0)
out of view	1.4609 (87.6)	0.0526 (3.15)	1.550 (93.0)
attenuation, dB	0.70	0.80	3.59
elevation (deg)	17.653	16.868	90
Rate (deg/sec) elevation azimuth	 0 -0.057	 0.1353 0.3495	 0.586 18.82

With maximum antenna rates from a separate run with 5 sec. increments

4.0 Outages For General Sun Synchronous Satellites

A large range of altitudes of sun synchronous satellites may be considered for use with a McMurdo Sound ground site. Low-altitude, low-cost satellites such as reported for a November 1994 Pegasus launch may be considered a prime opportunity for the McMurdo site. This section shows the variation in outage statistics as a function of altitude.

The inclination of sun synchronous satellites is actually function of altitude (Figure 4-1). This feature, along with the increased viewing region associated with high altitudes, has noticeable effects on outage times and viewing times. Long simulation can be done at each altitude and outage statistics extracted. Figure 4-2 shows the mean outage times ranging from 1.45 hours at 550 km altitude to 1.5 hours at altitudes slightly greater than 1000 km. Altitudes much less than 500 km, however, may actually skip an orbit before seeing McMurdo again. This appears as long outage time in Figures 4-2 and 4-3.

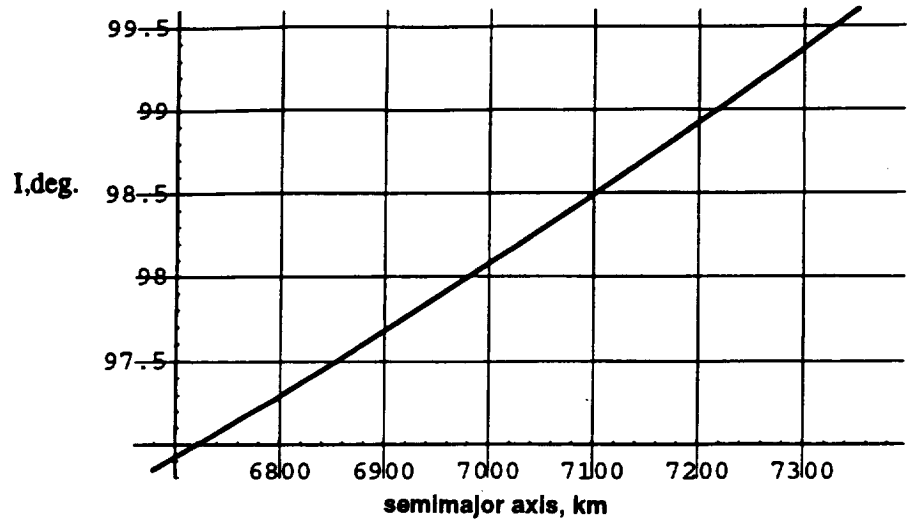

Figure 4-1: Required Inclination for Sun Synchronous Satellites

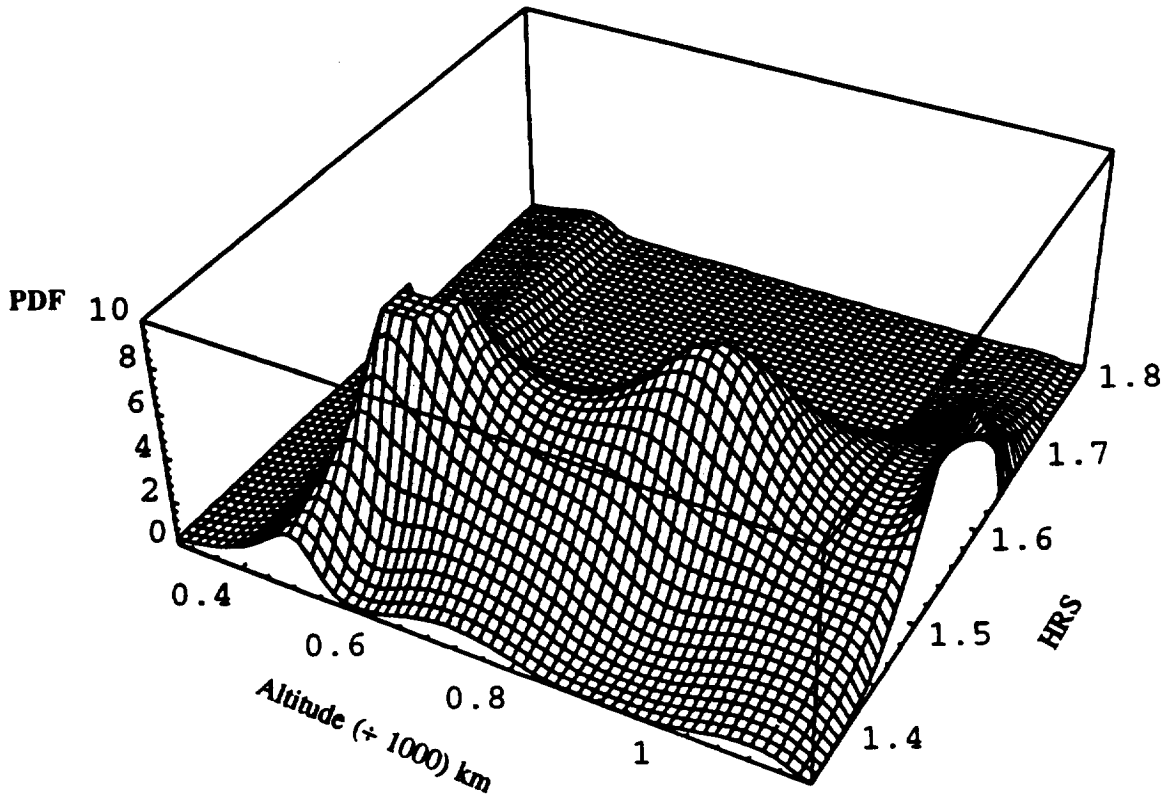

Figure 4-2: Outage PDF vs. Altitude1000

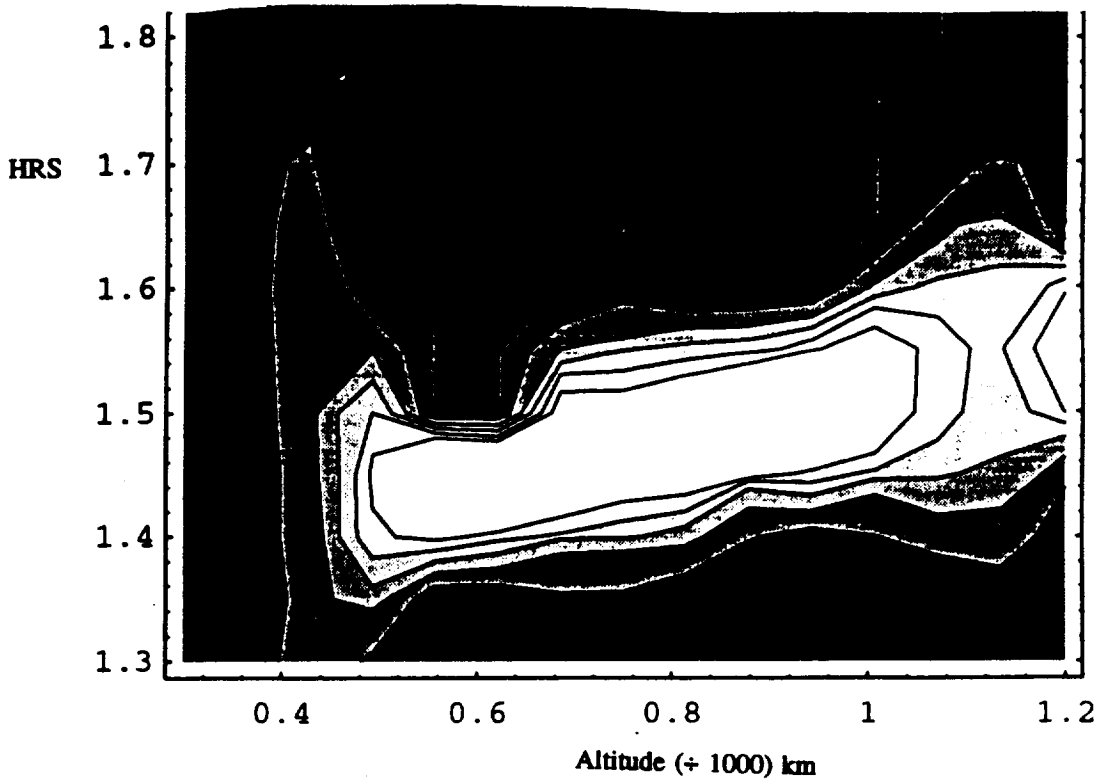

Figure 4-3: Contour Plot of Probability Density Function

Conclusions

We have discussed outage intervals, innage intervals, and dynamic propagation losses for a sun synchronous-McMurdo Sound ground site. Antenna rates have also been extracted from the link dynamics. McMurdo Sound has been shown to be an attractive ground site for a wide range of sun synchronous satellites from 500-1000 km altitude. EOS and Landsat were examined in detail. The observed 16-day Landsat periodicity was closely reproduced in the simulation. A unique elevation probability density function for McMurdo Sound was shown.

Acknowledgments

D. Thring of Stanford Telecom introduced legibility to the equations. J. Murphy pointed out, at the February 1996 AIAA Conference, that Analytic Graphics Inc. has also enjoyed a successful combination of speed and accuracy with the method of osculating elements.

Abbreviated References

[1] A. H. Jackson, P. Christopher, "Optimum Satellite Relay Positions," Proc. of Flight Mechanics and Estimation Symposium, NASA GSFC, May 1994.

[2] H. J. Liebe, P. W. Rosenkranz, and G. A. Hufford, "Atmospheric 60 GHz Oxygen Spectrum: New Laboratory Measurements and Line Parameters," J. Quantum Spectroscopy and Radiative Transfer, Vol. 48, No. 5/6, pp. 629-643, 1992.

[3] F. Moulton, "Celestial Mechanics," Macmillan, 1914.

[4] D. Brouwer, "Solution of the Problem of Artificial Satellite Theory Without Drag," Astron J., Vol. 64, No. 9, 1959, pp. 378-396.

[5] Y. Kozai, "The Motion of a Close Earth Satellite,", Astron J. Vol. 64, No. 9, 1959, pp. 367-377

[6] L. Blitzer, M. Weisfield, and D. Wheelon, "Perturbation of a Satellite Orbit Due to the Earth's Oblateness," J. Appl. Physics 27, No. 10, Oct. 1956, pp. 1141-1149.

[7] L. J. Ippolito, R. D. Kaul, and R. G. Wallace, "Propagation Effects Handbook for Satellite Systems Design," NASA Reference Publication 1082 (second edition), Dec. 1981.

[8] R. K. Crane, "Prediction of Attenuation by Rain," IEEE Transactions on Communications, Vol. Com 28, No. 9, September 1980.

[9] S.G. Lutz and G. Dorusheski, "Earth Antenna Beam Elevation Angles of Multiple-Access Satellite Communication Systems," Hughes Research Lab., Malibu, CA, Dept. 7, Contract NASW-495, August 1963.

[10] I. Sugai and P. Christopher, "Note on Distribution of Antenna Elevation Angles in Comsat System," IEEE Trans. on Aerospace and Electronic Systems (Corres.), Nov. 1967, pp. 981-982.

[11] A. K. Kamal, P. Christopher, "Communication at Millimeter Wavelengths," Proc. of International Communications Conference, Denver, June 1981.

[12] S. Wolfram, MATHEMATICA a System for Doing Mathematics by Computer, Second Edition, Adios Wesley Publishing Co., 1991.

APPENDIX A: CONDENSED ELEVATION ANGLE RECORD AT MCMURDO SOUND

A tabular output for ground antenna angles, times, and propagation loss is indispensable, and can be obtained from an April 1995 STel report. The figures below extract all the outage time to allow almost 1.7 days of EOS passes to be presented on each figure. They also allow a hypothetical 27 GHz downlink to be examined for atmospheric losses (11). Figure A-1 shows elevation angle vs time for the first 1.7 days. A quasi-cyclic period can be seen every day when very low elevation angles are seen at McMurdo. The elevation angles (data points) are read off the left scale. Atmospheric attenuation is read off the right scale.

Figures A-2 to A-10 extend the elevation angle record consecutively to 17.28 days.

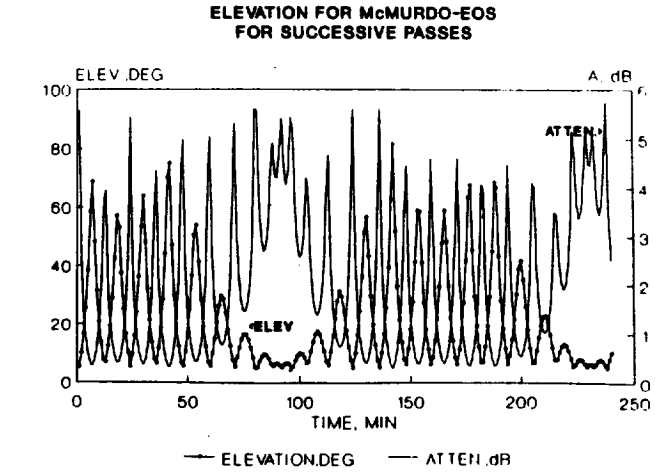

EXAMINE 27 GHz LINK LOSS AT P=0.997

A-1

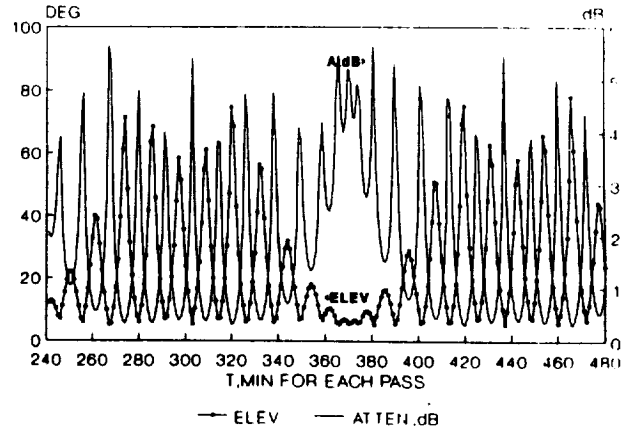

A-2

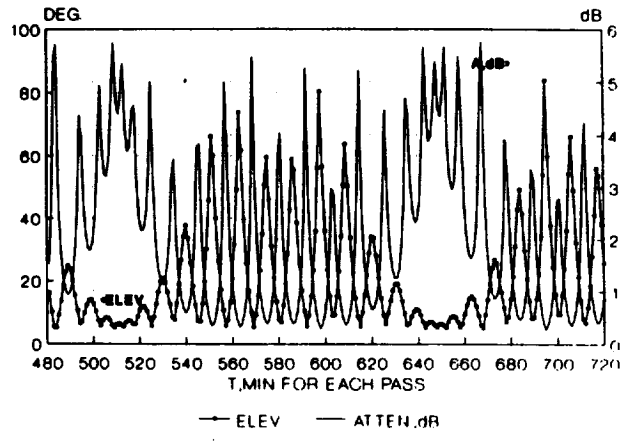

A-3

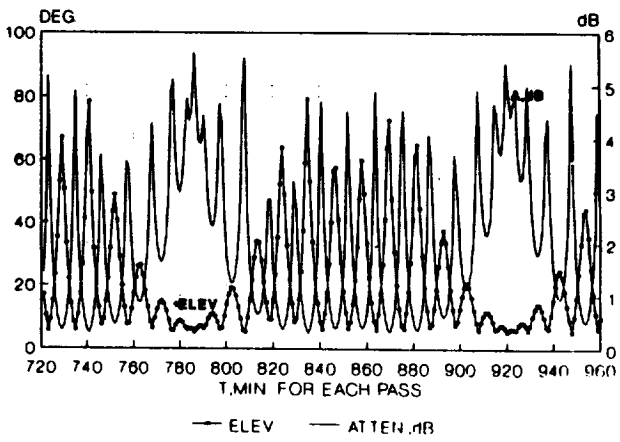

A-4

McMURDO PASSES;DAYS 8.98-8.63

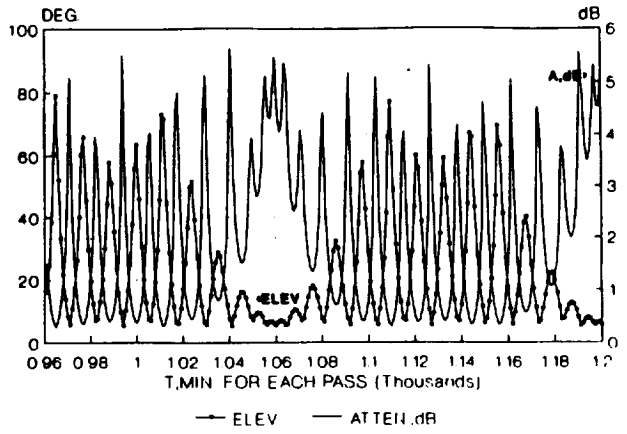

A-5

McMURDO PASSES;DAYS 8.63-10.34

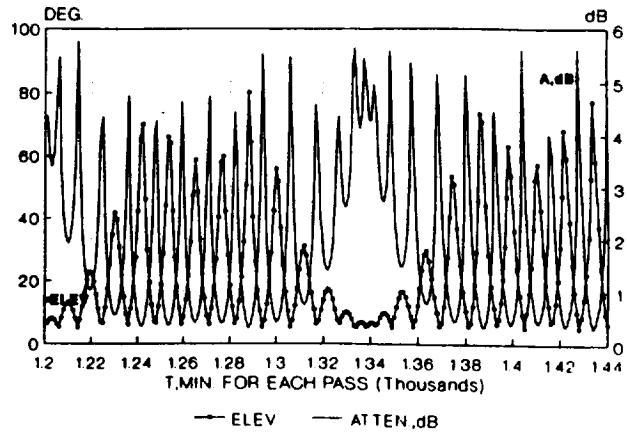

A-6

McMURDO PASSES;DAYS 10.34-12.07

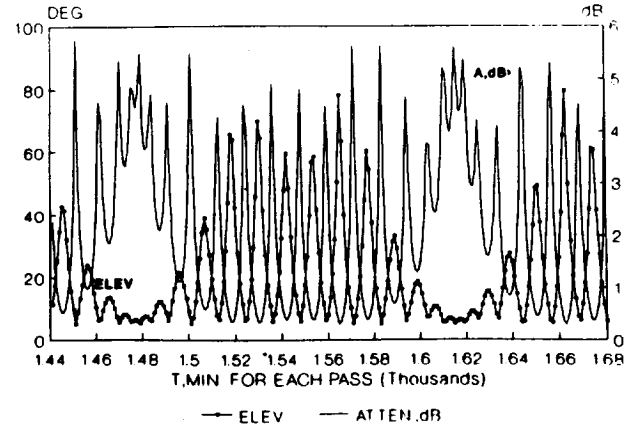

A-7

McMURDO PASSES;DAYS 12.1-13.9 DAYS

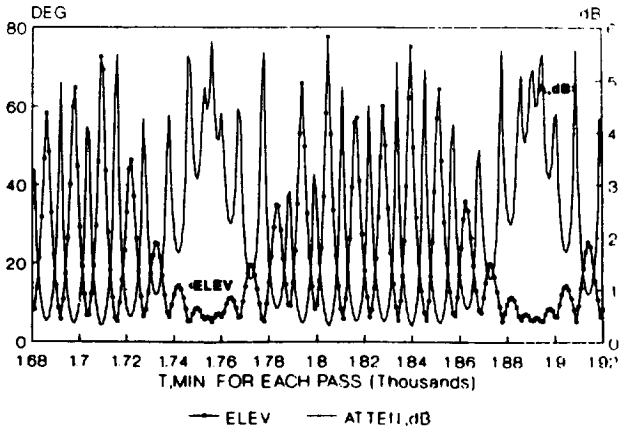

A-8

McMURDO PASSES;DAYS 13.9-15.56 DAYS

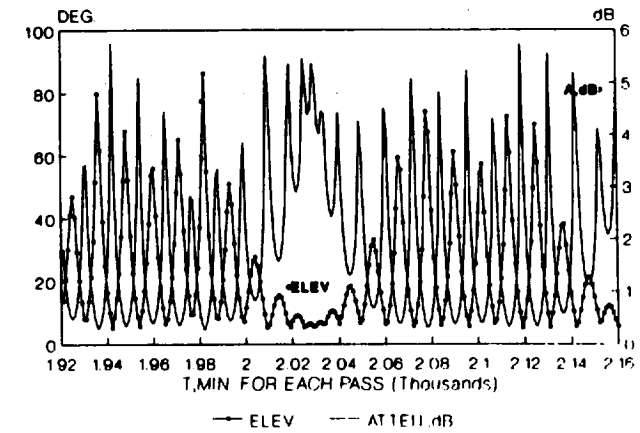

A-9

McMURDO PASSES;DAYS 15.56-17.28

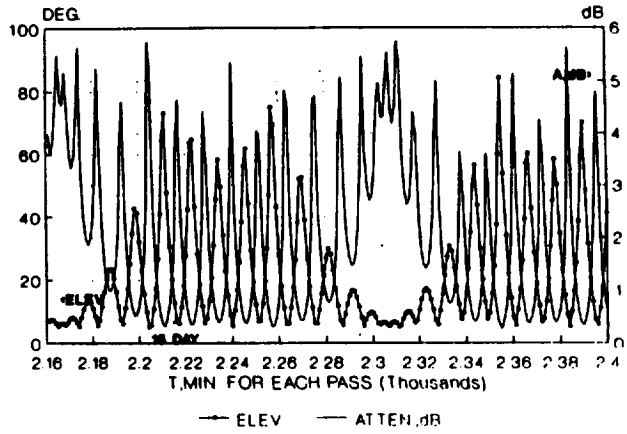

A-10

WR96039.A